Journal of Environmental Chemical Engineering 5 (2017) 5207–5214

Contents lists available at ScienceDirect

Journal of Environmental Chemical Engineering

journal homepage: www.elsevier.com/locate/jece

Metal-based mesoporous materials and their application as catalysts for the degradation of methyl orange azo dye

Sofía Schlichter[a], Karim Sapag[b], Mariana Dennehy[a], Mariana Alvarez[a,*]

[a] INQUISUR–Departamento de Química, Universidad Nacional del Sur, Avda. Alem 1253, 8000, Bahía Blanca, Argentina
[b] Laboratorio de Sólidos Porosos, LabSoP, INFAP, CONICET, Universidad Nacional de San Luis, 5700, San Luis, Argentina

ARTICLE INFO

Keywords:
Mesoporous catalysts
Cobalt
Manganese
Copper
Persulfate
Methyl orange

ABSTRACT

Cobalt, manganese and copper heterogeneous catalysts were prepared using MCM-41 and SBA-16 mesoporous supports. The synthesized materials were characterized by X-ray diffraction, chemical analysis, N_2 sorptometry, vibrational spectroscopy and transmission electron microscopy. Their catalytic activity was studied in the oxidative degradation of methyl orange (MO) in aqueous solution, at pH 6, using persulfate (PS) anion as oxidant at 30 °C. The level of degradation of the dye was monitored by UV–vis spectroscopy and Total Organic Carbon (TOC) analysis. The synthesized materials showed high activity, being the most effective catalysts those based on Co and Cu, achieving an efficient dye decolorization of > 95% until 2 h of reaction. After 24 h of reaction a high degree of mineralization was achieved (> 70%). Radical quenching studies showed that sulfate radicals are the main species formed by the catalyst/PS interaction. The supported catalysts exhibited stable performance during the reusability test, reaching an activity greater than 90% up to the fifth evaluated cycle of reuse for copper and cobalt based catalysts.

1. Introduction

A huge environmental hazard is being caused by the wastewater discharge from textile industries into water bodies. Among the various pigments that are discharged from textile industries, the azo dyes are the most frequently used. These substances, together with their intermediate and derivate products, such as aromatic amines, are mutagenic, carcinogenic and toxic to aquatic life and humans [1,2]. Thus, more attention has been recently focused on the development of new and efficient technologies for the degradation of these dyes before their release into the environment [3,4].

Numerous studies have included the use of catalysts in the degradation of pollutants [5,6]. Since Mobil Co. in 1992 firstly introduced ordered mesoporous MCM-41 and MCM-48 molecular sieves, they have been considered interesting materials for potential applications as adsorbents and catalyst supports [7,8]. The major advantages of these materials as catalytic supports are related to the unique combination of high surface area, pore volume, stability, very narrow-pore size distribution and the ease of separation and reuse [9,10]. Among them, SBA-16 seems to be one of the most remarkable structures; it has a 3D cubic arrangement of cage-like mesopores [11].

The isomorphous replacement of Si in pure siliceous material with metals strongly modifies the mesoporous materials properties. The replacement leads to modifications of the pore diameter and volumes, specific surface area and crystallographic parameters. However, the metal loading reached by a traditional hydrothermal synthesis is quite low [12,13]. In this sense, the surface functionalization of the mesoporous structures appears as an interesting alternative to produce catalysts with a higher metal loading. One of the methods of functionalization is based on silanizing the surface of a solid compound with 3-aminopropyltriethoxysilane, APTES. The silane group in APTES is highly reactive and silanizes the surface through the formation of covalent bonds with surface atoms. It is well known that functionalized hybrid materials are noteworthy since they associate in an unique solid phase both the properties of a rigid silica network and the particular chemical reactivity of the organic component [14,15].

Recently, Advanced Oxidation Processes (AOP) have gained great scientific interest worldwide. The principles of AOP are centered on the generation of radical species such as hydroxyl and sulfate radicals that can react with and destroy organic contaminants, producing innocuous carbon dioxide, water or other harmless by-products.

The use of persulfate ($S_2O_8^{2-}$) as an oxidant agent offers some advantages from other traditional oxidants (e.g. H_2O_2), such as high stability and solubility in water, low cost and ease of storage and

* Corresponding author.
E-mail addresses: sofia.schlichter@uns.edu.ar (S. Schlichter), sapag@unsl.edu.ar (K. Sapag), mdennehy@uns.edu.ar (M. Dennehy), alvarezm@criba.edu.ar, alvarezm72@yahoo.com.ar (M. Alvarez).

http://dx.doi.org/10.1016/j.jece.2017.09.039
Received 4 July 2017; Received in revised form 15 August 2017; Accepted 20 September 2017
Available online 28 September 2017

transport because of its solid state at room temperature. Even though the persulfate anion has an oxidation potential of 2.01 V, its activation is required to improve degradation ability. From all the activation techniques [16–19], transition metal ions activation is particularly attractive [20,21]. The activation produces the sulfate free radical ($SO_4\cdot^-$) which is a strong one-electron (E^o = 2.5–3.1 V) oxidant [22] that produces a rapid and deep oxidation of many organic compounds.

To our knowledge, scarce reports appear in the literature regarding the use of metal-functionalized mesoporous supported catalysts, based on transition metals like Co, Cu and Mn for the degradation of azo dyes employing AOPs. Moreover, high metal loading applying the use of direct impregnation in these types of catalysts is not achieved in the existing reports. In order to explore the use of these materials, in this work, manganese, cobalt and copper-based catalysts were prepared using mesoporous materials (MCM-41 and SBA-16) as supports, following two different methodologies. One of the methodologies employed was focused on the surface modification of MCM-41 or SBA-16 by reaction with a spacer, namely 3-aminopropyltriethoxysilane (APTES), followed by metal coordination to the nitrogen groups of the spacer. The other one was based on the direct interaction between the support and the metal cation. The catalysts were fully characterized and their catalytic activity was tested in the oxidative degradation of methyl orange (Sodium 4-[(4-dimethylamino) phenyldiazenyl]benzenesulfonate), a monoazodye, using $S_2O_8^{2-}$ as the oxidizing agent.

2. Materials and methods

2.1. Synthesis of supports

All the reagents were of analytical grade and were used as received without further purification

2.1.1. MCM-41

The hexagonal MCM-41 was prepared following the specifications of Bore et al. [23]. The synthesis involved the dissolution of cetyltrimethyl ammonium bromide (CTAB) surfactant in water and the addition of sodium silicate as the silica source (SiO_2 27%, NaOH 10%, H_2O 63%) in a batch reactor. The molar ratio of the precursor solution was $3.4SiO_2$:1CTAB:$286H_2O$. The pH of the mixture was adjusted to 10 with 1 M HNO_3. It was kept in a water bath under static conditions for 8 h at 80 °C. Then, the mixture was cooled to room temperature. The powder was washed with double distilled water and vacuum filtered.

2.1.2. SBA-16

Cubic SBA-16 was synthesized by the conventional hydrothermal pathway. The procedure described by Van Der Voort et al. [24] was followed. Pluronic F127 (4 g) was dissolved in 30 g of double distilled water at room temperature, followed by the addition of 120 mL of 2 M HCl solution, under mechanical stirring. Then, 5.75 mL of tetraethyl orthosilicate (TEOS) were added. Once a homogeneous solution was obtained, the mixture was stirred for 20 h at room temperature. At that time the sample was aged in an oven at 100 °C for 48 h. The solid was washed with double distilled water, filtered and dried in air.

2.2. Preparation of the catalysts

2.2.1. Mesoporous supports functionalization

Mesoporous MCM-41 and SBA-16 were functionalized by a post-synthesis grafting method using 3-aminopropyltriethoxysilane (APTES, Scheme 1) by means of the modified technique proposed in [25]. For that, the surfactant of the as-synthesized samples was removed by calcination at 550 °C (6 h, 1 °C min^{-1} for MCM-41, 9 h, 2 °C min^{-1} for SBA-16). After that, ca. 3 g of mesoporous materials were pretreated in oven at 110 °C overnight and immersed in solution of 135 mL of dry toluene and 13.5 mL of APTES. The mixture was kept under reflux for 8 h at 110 °C in nitrogen atmosphere. Then, the toluene was evaporated and the solids were washed three times with chloroform. The functionalized materials were denoted as MCM-41-NH2 and SBA-16-NH2.

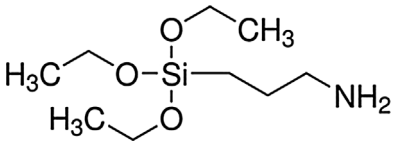

Scheme 1. Structure of APTES.

The loading of transition metal ions on the functionalized supports was carried out as follows: 20 mL of 0.15 M $MeSO_4$ solution (Me = Co^{2+}, Cu^{2+} or Mn^{2+}) were added to 500 mg of solid support. The mixture was kept for 24 h under mechanical stirring at room temperature [26]. The solid was centrifuged, washed with double distilled water and dried at room temperature. The products were denoted as Me/MCM-41-NH2 and Me/SBA-16-NH2 (Me = Co, Mn, Cu).

2.2.2. Direct metal impregnation

To evaluate a new method to upload the transition metal onto mesoporous support a new catalyst based on MCM-41 was synthesized. In this case, the addition of copper in the mesoporous matrix was conducted by impregnation. MCM-41 was employed as-synthesized, without eliminating the structure-directing agent. The sample was prepared contacting 1.0 g of MCM-41 with 5 mL of a solution of copper acetylacetonate ($Cu(AcAc)_2$) in toluene at 70 °C under continuous stirring for 24 h [12]. The target Cu concentration in the solution was 24 wt%. Subsequently, the material was dried at 70 °C for 4 h and calcined at 400 °C for 6 h (0.5 °C/min) in order to remove the surfactant. The sample was named Cu/MCM-41-24.

2.3. Catalysts characterization

The metal content of the obtained catalysts was determined by atomic absorption spectroscopy (AAS) using a GBC Avanta Model B-932. X-ray diffraction (XRD) patterns were collected on a Philips diffractometer PW1710 BASED (45 kV, 30 mA) with a $CuK\alpha_1$ radiation (1.5406 Å) and a graphite monochromator. Fourier-Transform infrared (FTIR) spectra of the samples were recorded in a FTIR-NIR Thermo Scientific Nicolet iS50, in the 400–4000 cm^{-1}region. The samples were dispersed in KBr disks. Transmission electron microscopy (TEM) images were obtained using a JEOL 100 × 2 (Tokyo, Japan) apparatus. Textural properties of the catalysts were determined from nitrogen adsorption–desorption isotherms data at −196 °C obtained on AUTOSORB-1MP. The specific surface areas were calculated using Brunauer, Emmett and Teller method (BET).

2.4. Analytical method

The UV–vis spectra of MO were recorded from 200 to 800 nm with a UV/Vis spectrophotometer (Cecil 2021). The maximum absorbance wavelength (λ_{max}) of MO was found at 464.5 nm, at pH 6.

2.5. Degradation of MO

The degradation reactions were carried out in a thermostatized beaker glass, at 30 °C. The reaction tests were run in duplicate. In a typical procedure 150 mL of MO solution (10 mg L^{-1}, pH 6) were added to the beaker. The reaction was initiated by adding 30 mg of $K_2S_2O_8$ and 200 mg of the catalyst under continuous stirring. These experimental conditions were selected according to the literature and considering the optimal conditions for MO degradation [27,28]. At designated sampling intervals and up to 2 h of reaction, 3 mL aliquots were withdrawn and filtered through a Nuclepore membrane(pore size 0,22 μm) using a syringe. Decolorization extents were established by measuring the absorbance in visible spectra at the characteristic

wavelength of the MO. The percentage of degradation of MO was calculated as follows:

$$\text{Degradation } (\%) = \left(1 - \frac{C_t}{C_0}\right) \times 100$$

where C_0 was the initial concentration of MO (mg L^{-1}) and C_t was the concentration of the aliquot at time t (mg L^{-1}). All the degradation experiments were carried out in duplicate and the averages were reported.

The mineralization of MO solution was established on the basis of total organic carbon (TOC) content, performed by using a TOC-$L_{CPH/CPN}$ analyzer (Shimadzu). The pH was monitored with an Orion 250Aplus pH meter equipped with a pH electrode.

The leaching of Co, Cu and Mn ions in the residual solutions were also determined with a GBC Avanta B-932 Atomic Absorption Spectrometer.

The effect of the visible light on the degradation was also evaluated, together with a blank reaction involving decolorization of MO with PS in absence of catalysts. The efficiency of the decolorization of MO using catalysts without PS was also analyzed.

Two sets of quenching experiments were performed to determine the radical species formed by the metal-oxidant couple. The experimental procedures were repeated as previously with the addition of *tert*-butyl alcohol (TBA) and ethanol (EtOH). A specific amount of each alcohol was added in the reactor before the catalyst and the oxidant addition to obtain a 600:1 molar ratio of the alcohol versus the oxidant.

2.6. Catalyst reusability

The reusability of the catalysts up to five successive recycles was studied in MO degradation, under the same reaction conditions. For that, at the end of the reaction the solid was immediately washed with double distilled water and dried in an oven at 30–40 °C. This cycle was repeated five times, keeping constant the PS:MO:catalyst ratio.

3. Results and discussion

3.1. Characterization of the catalysts

The XRD profile of the MCM-41 sample shows a typical pattern of the hexagonal mesoporous structure (Fig. 1a). An intense peak at low 2θ angle attributable to the diffraction of (100) plane is detected. In addition, other minor peaks related to (110), (210) and (200) reflections planes are observed.

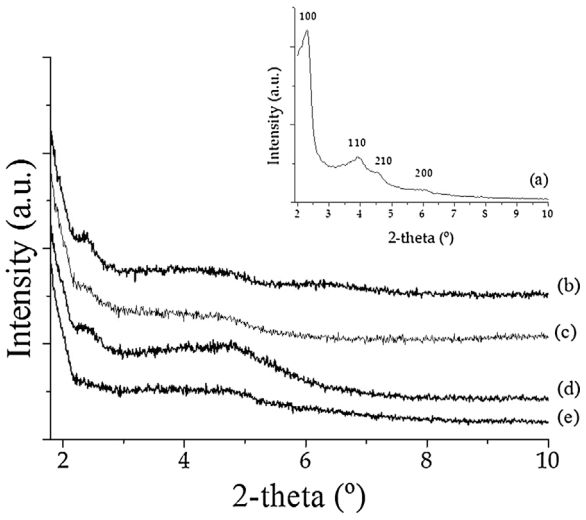

Fig. 1. X-Ray diffraction patterns of (a) MCM-41 parent (inset), (b) functionalized support, (c) Cu/MCM-41-NH2, (d) Mn/MCM-41-NH2, (e) Co/MCM-41-NH2.

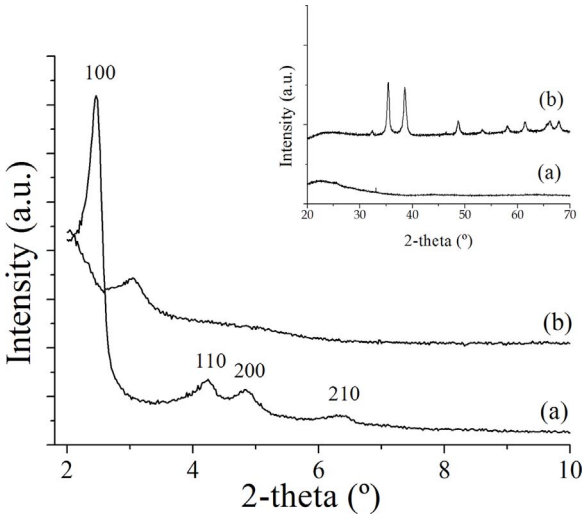

Fig. 2. X-Ray diffraction patterns of (a) MCM-41 parent and (b) Cu/MCM-41-24.

On the contrary, the XRD patterns of the functionalized material (Fig. 1b) and the corresponding metal catalysts Cu/MCM-41-NH2 (Fig. 1c), Mn/MCM-41-NH2 (Fig. 1d) and Co/MCM-41-NH2 (Fig. 1e) show a significant decrease in the intensity of the diffraction peaks, probably due to a partial collapse of the structure of the ordered phase MCM-41.

The XRD profile of the sample obtained by impregnation of MCM-41 with $Cu(AcAc)_2$ shows that the catalyst retain the mesoporous structure (Fig. 2b). Low angle peak is conserved, thought with lower intensity. In addition to MCM-41 peaks, characteristic peaks of CuO (2θ = 35.4°, 38.8°) appear in the high-angle region of the XRD pattern (Fig. 2, inset).

The metal loading of the samples, as measured by AAS, together with their SSA values are presented in Table 1.

Fig. 3 shows the TEM images of free MCM-41 (Fig. 3a) and SBA-16 (Fig. 3b). MCM-41 exhibits a hexagonal array of channels while SBA-16 displays well-ordered cubic array of mesostructure and shows the presence of 3-D channels running along the mesopores. In the case of Cu/MCM-41-24 (Fig. 3c) a reduction in the order after the addition of the metal is seen, although the mesoporous order is retained. These results are in accordance with those obtained by XRD.

On the other hand, the long-range regularity of SBA-16 and MCM-41 mesopores somehow lowered down after the functionalization.

FTIR measurements were performed in order to characterize the silica-based matrices, and in particular, the incorporation of organic functions to the pore systems. The FT-IR spectra of parent MCM-41, functionalized MCM-41-NH2 and the two copper-based catalysts (Cu/MCM-41-NH2 and Cu/MCM-41-24) are shown in Fig. 4. All spectra present the typical Si—O—Si bands of the inorganic framework in the 800 cm^{-1} and in the 950–1300 cm^{-1} region [29–31]. The absorbance of the Si—O—H bands at 960 cm^{-1} in parent MCM-41 turns into a shoulder upon functionalization, indicating that the surface silanols were substituted by aminosilane groups. The presence of organic groups is confirmed by bands in the 2800–3000 cm^{-1} region, mainly

Table 1
Metal content and specific surface areas values of the mesoporous catalysts.

Sample	Metal Content (weight%)			SSA ($m^2\ g^{-1}$)
	Co	Cu	Mn	
MCM-41	–	–	–	1100
Co/MCM-41-NH2	17.0	–	–	125
Cu/MCM-41-NH2	–	14.0	–	9
Mn/MCM-41-NH2	–	–	17.7	85
Co/SBA-16-NH2	1.7	–	–	385
Cu/SBA-16-NH2	–	4.1	–	210
Cu/MCM-41-24	–	19.0	–	864

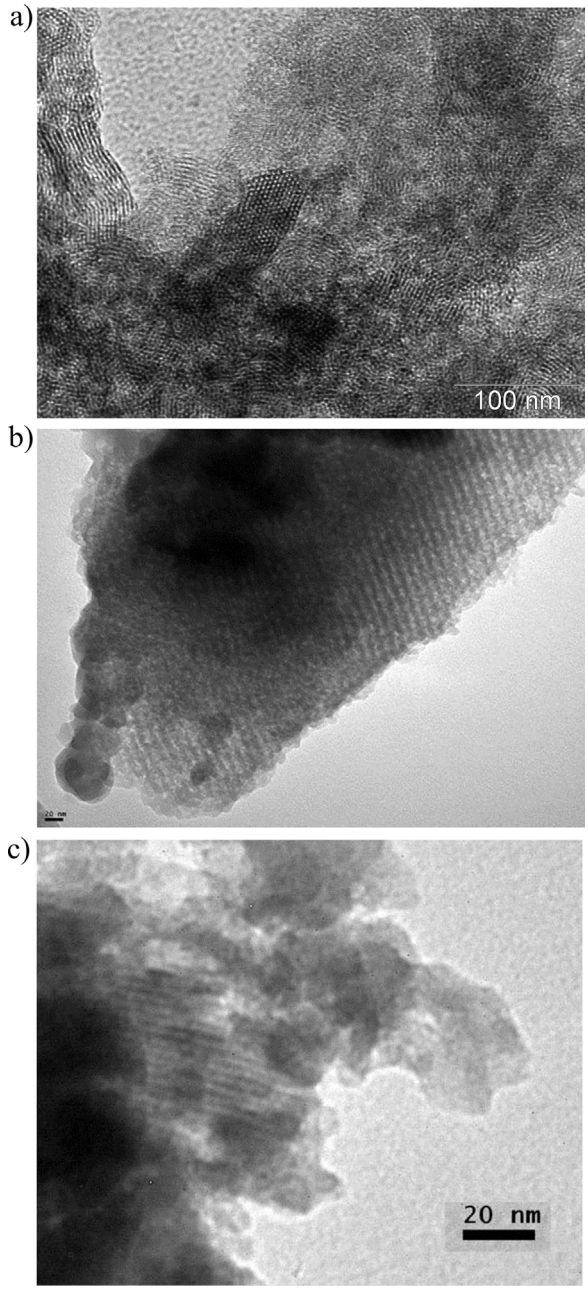

Fig. 3. TEM images of free (a) MCM-41 and (b) SBA-16. (c) Cu/MCM-41-24.

attributed to the symmetric stretching modes of methyl and methylene groups. The N—H and C—H stretching vibrations of APTES are observed in the region 3500–3000 cm^{-1} (superimposed to those of water), respectively, and the corresponding H—N—H and H—C—H bending vibrations can also be observed in the regions 1700–1500 cm^{-1} and 1500–1300 cm^{-1} [32]. Several changes compared to the parent material appeared in the characteristic regions of APTES groups, attributable to the metal-APTES interaction. Cu/MCM-41-24 spectrum seems to be very similar to the bare support.

Similar IR profiles were obtained for the SBA-16 based catalysts (Supplementary material).

3.2. Catalytic activity

Preliminary experiments were carried out in order to evaluate the individual effect of catalysts and PS on the MO removal, including adsorption of dye molecules on the catalyst surface and non-catalytic

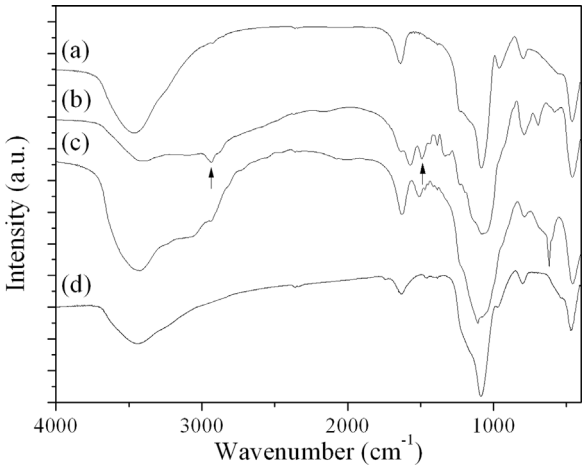

Fig. 4. FT-IR spectra in the 400–4000 cm^{-1} region of (a) MCM-41, (b) MCM-41-NH2 and (c) Cu/MCM-41-NH2 (d) Cu/MCM-41-24.

chemical oxidation with PS. A control test using only PS showed less than 40% color removal was reached after 2 h reaction time. Another experiment, using the aminated material MCM-41-NH2 was also carried out, and the degradation profiles were practically identical, corroborating the inaction of the support. On the other hand, when the functionalized SBA-16 support was tested, a higher percentage of MO decolorization was reported, but the removal could be mainly attributed to adsorption of the dye over the solid. Besides, for the purpose of verifying the influence of the light over the MO degradation, the reaction was also performed in the dark using selected catalysts. The kinetic profiles were practically identical, showing that the reaction was not photo-catalyzed.

Results illustrated in Fig. 5 show that the simultaneous presence of heterogeneous catalyst and PS led to significant enhancement of the MO oxidation rate as compared to the adsorption and oxidation with PS but without catalyst. All the synthesized materials were able to degrade the MO molecule in the studied conditions (30 °C, pH 6) and showed a high conversion level at 120 min of reaction. Color loss is attributed to the breakdown of nitrogen double bond, —N═N— (azo) in the molecule, by the $SO_4\cdot^-$ radical generated from the persulfate anion. Among all the tested samples, the best catalytic performance was attained with Co/MCM-41-NH2 and Cu/MCM-41-NH2- (> 90% after 120 min of reaction), while for Mn/MCM-41-NH2 and Cu/MCM-41-24, decolorizations of around 60% were obtained.

In addition, with the aim of verifying if the decolorization process was conducted by adsorption or degradation, the IR spectra of the catalysts were recorded before and after the reaction. For practical purposes only the IR spectra of the Cu-based catalysts are presented in Fig. 6, together with the spectrum of the azo dye.

The characteristic bands of MO were not found on the oxide surface after the decolorization reaction. Thus, these results could indicate that the faster and complete removal of MO from the solution under heterogeneous oxidation mode is due to its catalytic transformation rather than the physical, nondestructive adsorption of the dye molecules on the catalyst surface

The residual solutions of MO were colorless after 2 h of reaction using Cu/MCM-41-NH2 and Cu/SBA-16-NH2. However, the residual solution of the experience tested with Cu/MCM-41-24 was slightly colored after that time. The UV–vis spectra of these solutions and those collected after 24 h of reaction are shown in Fig. 7. As a comparison, the spectrum of the dye is also presented. The spectrum of MO exhibits a broad band at 465 nm typical of a substituted azobenzene, and a band in the UV at 271 nm, corresponding to π-π* transitions of benzene groups. When the experience was carried out only in the presence of persulfate (without catalyst addition) the spectrum of the residual

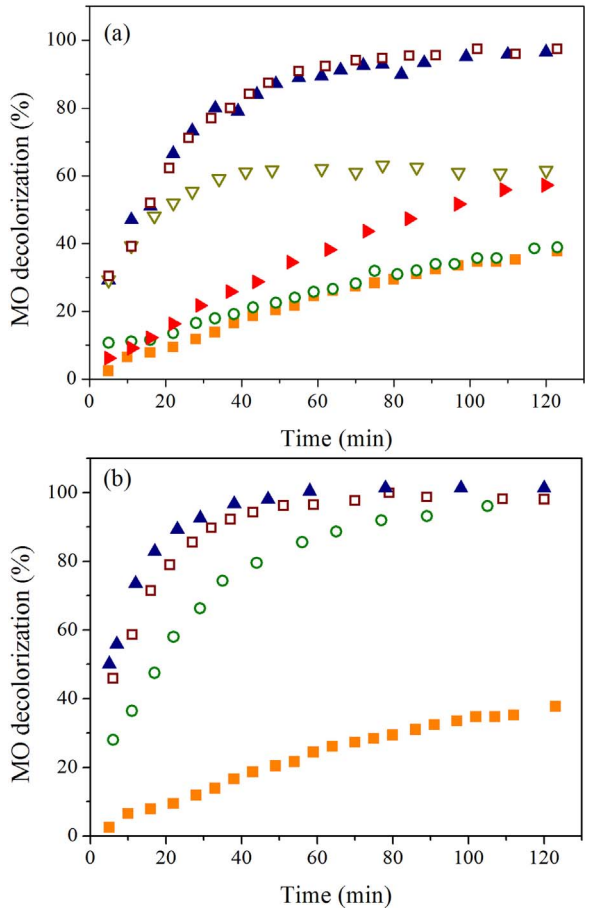

Fig. 5. Percentage of decolorization of MO with: (a) PS alone (■), MCM-41-NH2 (◯), Co/MCM-41-NH2 (▲), Mn/MCM-41-NH2 (▽), Cu/MCM-41-NH2 (□), Cu/MCM-41-24 (▶); (b) PS alone (■), SBA-16-NH2 (◯),Cu/SBA-16-NH2 (□), Co/SBA-16-NH2 (▲).

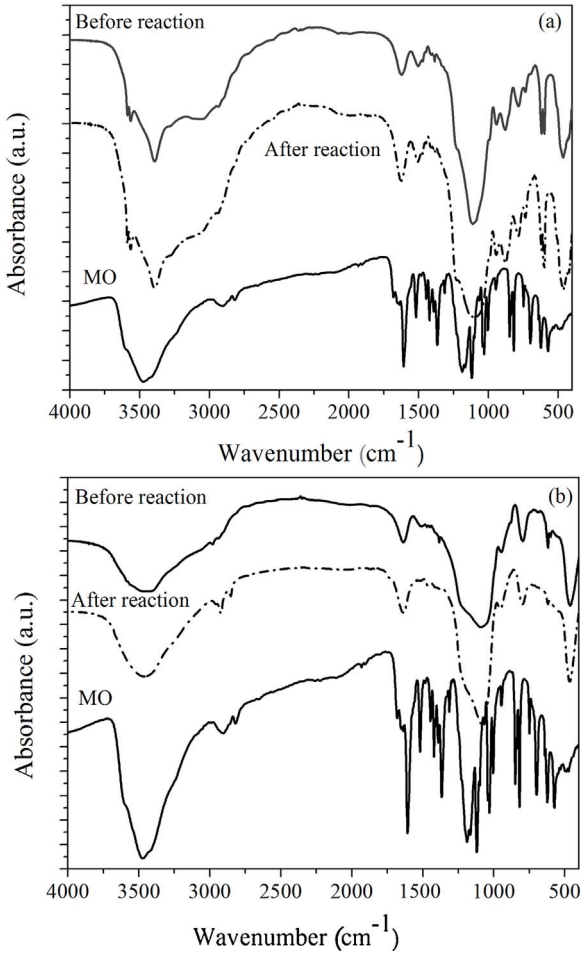

Fig. 6. IR spectra of Cu-based catalysts before and after reaction (a) Cu/MCM-41-NH2, (b) Cu/SBA-16-NH2.

solution showed that the characteristic bands of MO decreased in intensity, but persisted even after 48 h of reaction (Fig. 7). When Cu/MCM-41-NH2 and Cu/SBA-16-NH2 were tested, all the bands disappeared within 24 h while for Cu/MCM-41-24 low-intensity bands corresponding to benzene groups were found in the residual solution.

To investigate the possibility of homogeneous phase reaction promoted by metal species solubilized from the catalysts, atomic absorption analyses were carried out on the residual liquids after the reaction, which showed no significant leaching of the metals to the solution (< 1%).

The TOC removal efficiency was studied, since it is a good indicator for mineralization of organic species. Surprisingly and in spite of the UV–vis spectrum obtained for Cu/MCM-41-24, TOC decreased rapidly to 53% removal in the first 2 h of reaction and continued decreasing up to 70% after 6 h. The TOC removal efficiency for functionalized catalysts was not as good as the last one and this might be due to damage to the catalyst caused by radicals.

In addition, the temperature is also a key factor influencing catalyst activity on MO degradation. Fig. 8 shows the effect of temperature on MO degradation using copper catalysts. As it was expected, higher MO removal was obtained at increased temperature. For instance, for Cu/MCM-41-NH2, the highest removal of MO was achieved in ca. 80 min at 30 °C, while at 40 °C and 50 °C, the highest removal of the dye was attained in 60 min and 40 min, respectively. The same trend was also observed foe the Cu/SBA-16-NH2 catalyst.

In order to estimate the kinetic rates at different temperatures, several kinetic models were tested. MO degradation curves best fitted to the first-order kinetics:

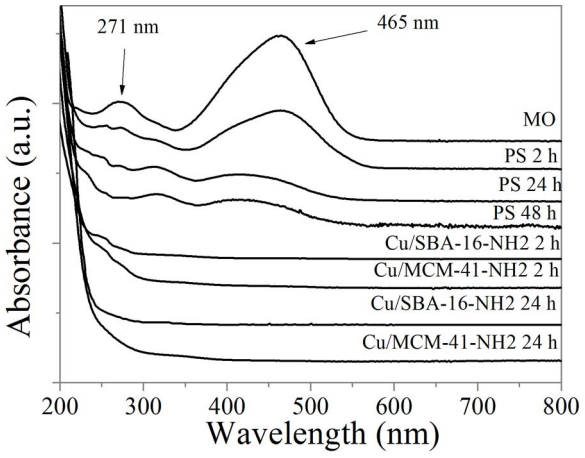

Fig. 7. UV–vis spectra of degradation of MO over PS alone, and PS together with Cu/supported catalysts.

$$ln\left(\frac{C}{C_0}\right) = -kt$$

where C is MO concentration at time (t) and C_0 is the MO concentration at initial time (t_0) and k is the first order reaction rate constant (min^{-1}). The high values of regression coefficients and kinetic constants are presented in Table 2. For comparison purposes, kinetic rate constants for experiments conducted with PS alone, without catalyst, are also shown.

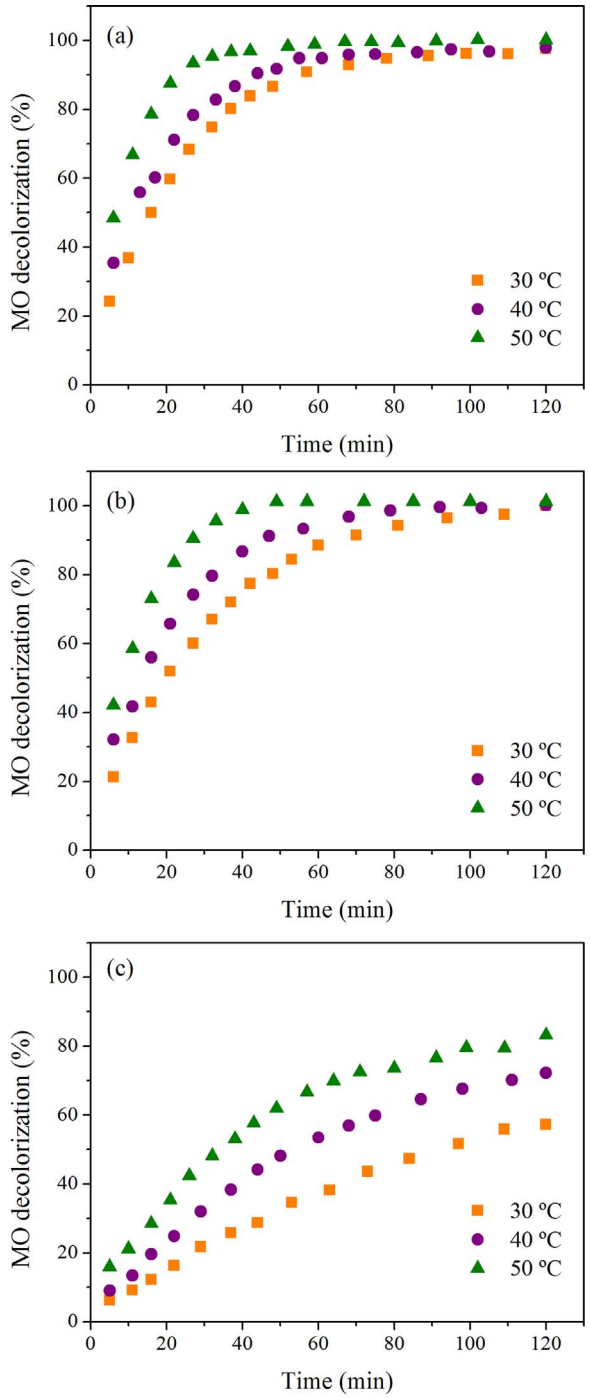

Fig. 8. Effect of the temperature on the degradation of MO using (a) Cu/MCM-41-NH2, (b) Cu/SBA-16-NH2 and (c) Cu/MCM-41-24.

As it was expected, the kinetic rate of reaction increased with increasing temperature. The activation energy was determined by the Arrhenius equation:

$$k = A\ \exp^{-\frac{E_a}{RT}}$$

where A is the frequency factor, E_a is the activation energy, R is the universal gas constant and T is the absolute temperature. The Arrhenius plot of ln (k) vs 1/T for Cu/MCM-41-NH2 presented a good linear correlation (R^2: 0.98) and the activation energy was derived as 29 kJ/mol. Furthermore, the activation energy for Cu/SBA-16-NH2 was around 42 kJ/mol (R^2: 0.98). The lowest activation energy was found with Cu/MCM-41-24 (28 kJ/mol, R^2: 0.98). These values confirm that

Table 2
Kinetic constants of MO degradation at different temperatures on Cu-based catalysts.

Sample	Temperature (°C)	k (min^{-1})	R^2
PS (no catalyst)	30	0.003	0.98
	40	0.005	0.99
	50	0.009	0.98
Cu/MCM-41-NH2	30	0.037	0.99
	40	0.048	0.99
	50	0.076	0.98
Cu/SBA-16-NH2	30	0.035	0.99
	40	0.051	0.99
	50	0.094	0.99
Cu/MCM-41-24	30	0.007	0.99
	40	0.011	0.99
	50	0.014	0.98

the catalysts decrease the activation energy of the degradation reaction of MO with PS (the activation energy for PS alone was 46 kJ/mol, R^2: 0.99). To our knowledge there are no comparable measurements in the literature. However, our results are similar or even lower than those found in similar systems, for example for the catalytic decolorization of Acid Blue 29 dye by H_2O_2 using a copper-based catalyst [33]. Yao et al. [34] reported a Mn_3O_4/graphene system in activation of PMS for Orange II degradation and found the activation energy at 49.5 kJ/mol. Investigations on Co-based systems for Orange II azo dye and phenol degradation showed that activation energies of supported Co catalysts are in the range of 47–50 kJ/mol [35–37].

To identify the primary radical species formed by the metal catalyst and the oxidant interaction, quenching experiments were conducted with selected copper catalyst with the addition of TBA and EtOH. Anipsitakis and Dionysiou [38] suggest that alcohols containing α-hydrogen, such as ethanol, react at high and comparable rates with hydroxyl and sulfate radicals ($k_{EtOH/\cdot OH} = 1.2 \times 10^9 - 2.8 \times 10^9\ M^{-1}\ s^{-1}$; $k_{EtOH/SO4\cdot -} = 1.6 \times 10^7 - 7.7 \times 10^7\ M^{-1}\ s^{-1}$). Moreover, although alcohols with no α-hydrogen such TBA are effective quenching agents for hydroxyl radicals, they react much slower with sulfate radicals, being the reaction rate with hydroxyl radicals approximately 1000-fold greater than that with sulfate radicals ($k_{TBA/\cdot OH} = 3.8 \times 10^8 - 7.6 \times 10^8\ M^{-1}\ s^{-1}$; $k_{TBA/SO4\cdot -} = 4.0 \times 10^5 - 9.1 \times 10^5\ M^{-1}\ s^{-1}$). Based on these properties, the effect of the presence of TBA is much more critical, rather than that of EtOH, and the change in the transformation of the substrate due to the addition of TBA allowed us to differentiate between sulfate and hydroxyl radicals. The transformation of MO by Cu/MCM-41-NH2 catalyst was affected by the presence of TBA or EtOH since almost 20% less of transformation was achieved in both cases. From these data, it is concluded that the major species formed from the Cu/MCM-41-NH2 and PS interaction are $SO_4\cdot^-$, and hence those radicals could be responsible for the transformation of the substrate.

The evaluation of the reusability of the obtained catalysts is essential because the long-term stability is an important property for effective catalysts and is crucial for its practical application. Therefore, several successive batch runs of the MO degradation reaction were conducted by using selected the recycled catalysts under the tested reaction conditions and keeping constant the PS:catalyst:MO ratio. For that, the catalyst was recovered from the reaction mixture after each run, washed thoroughly with double distilled water and dried overnight before the next run. The results are presented in Fig. 9.

As can be seen, the Cu- and Co-based catalysts kept the capacity of degradation after all the studied cycles. For the Mn catalyst, on the other hand, the percentage of degradation increased from 55 to around 90% in the first reuse, and this efficiency value was maintained up to 3 cycles of reuse. Saputra et al. [39] synthesized and tested a series of manganese oxides with different oxidation states in the heterogeneous activation of peroxymonosulfate for phenol degradation in aqueous solutions. Among them, Mn_2O_3 resulted to be the most effective catalyst

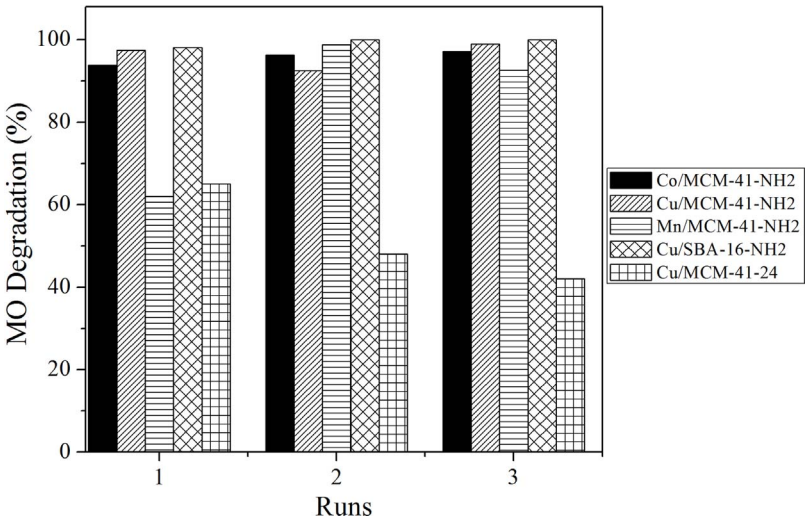

Fig. 9. Reusability of the obtained catalysts.

for generating sulfate radicals to degrade phenol, and the authors related their catalytic activity to the redox potential. Therefore, the behavior of the Mn/MCM-41-NH2 catalyst could be attributed to a change in the oxidation state of the Mn^{2+} after the first catalytic test, giving rise a more reactive superficial species of manganese, available for posterior cycles.

4. Conclusions

Heterogeneous Co, Cu and Mn catalysts supported on MCM-41 and SBA-16 were synthesized and fully characterized, and the catalytic activity of these materials in the oxidative degradation of MO in aqueous solution at pH 6 and 30 °C was tested. The synthesized materials showed high activity, being the most effective catalysts those based on Co and Cu, achieving an efficient dye removal of > 95% until 2 h of reaction.

In some cases, after 24 h of reaction a high degree of mineralization was achieved (> 70%). Radical quenching studies demonstrated that sulfate radicals are the main species formed by the catalyst/PS interaction and hence those that are responsible for the degradation of the MO in solution. The supported catalysts obtained by impregnation also exhibited stable performance during the reusability test.

Acknowledgements

The authors gratefully acknowledge Lic. Rodolfo Dionisi and Lic. Claudio Vanina for their generous cooperation in the TOC measurements. This project was supported by SGCyT -UNS (Project M24/Q075).

Appendix A. Supplementary data

Supplementary data associated with this article can be found, in the online version, at http://dx.doi.org/10.1016/j.jece.2017.09.039.

References

[1] K.T. Chung, S.E. Stevens, Degradation azo dyes by environmental microorganisms and helminths, Environ. Toxicol. Chem. 12 (1993) 2121–2132.
[2] M.S. Lucas, J.A. Peres, Decolorization of the azo dye R Reactive Black 5 by Fenton and photo-Fenton oxidations, Dyes Pigm. 71 (2006) 236–244.
[3] S. Vanhulle, M. Trovaslet, E. Enaud, M. Lucas, S. Taghavi, D.V.D. Lelie, B.V. Aken, M. Foret, R.C.A. Onderwater, D. Wesenberg, S.N. Agathos, Y.J. Schneider, A.M. Corbisier, Decolorization cytotoxicity, and genotoxicity reduction during a combined ozonation/fungal treatment of dye-contaminated wastewater, Environ. Sci. Technol. 42 (2008) 584–589.
[4] D. Valero, J.M. Ortiz, E. Expósito, V. Montiel, A. Aldaz, Electrochemical wastewater treatment directly powered by photovoltaic panels: electrooxidation of a dye-containing wastewater, Environ. Sci. Technol. 44 (2010) 5182–5187.
[5] Sheng-Peng Sun, Cheng-Jie Li, Jian-Hui Sun, Shao-Hui Shi, Mao-Hong Fan, Qi Zhou, Decolorization of an azo dye Orange G in aqueous solution by Fenton oxidation process: effect of system parameters and kinetic study, J. Hazard. Mater. 161 (2009) 1052–1057.
[6] G.B. Ortiz de la Plata, O.M. Alfano, A.E. Cassano, Optical properties of goethite catalyst for heterogeneous photo-Fenton reaction. Comparison with a titanium catalyst, Chem. Eng. J. 137 (2008) 396–410.
[7] C.T. Kresge, M.E. Leonowicz, W.J. Roth, J.C. Vartuli, J.S. Beck, Ordered mesoporous molecular sieves synthesized by a liquid-crystal template mechanism, Nature 359 (1992) 710–712.
[8] B.P. Ajayi, B. RabindranJermy, K.E. Ogunronbi, B.A. Abussaud, S. Al-Khattaf, n-Butane dehydrogenation over mono and bimetallic MCM-41 catalysts under oxygen free atmosphere, Catal. Today 204 (2013) 189–196.
[9] Y. Dong, X. Zhan, X. Niu, J. Li, F. Yuan, Y. Zhu, H. Fu, Facile synthesis of Co-SBA-16 mesoporous molecular sieves with EISA method and their applications for hydroxylation of benzene, Microporous Mesoporous Mater. 185 (2014) 97–106.
[10] K.P. Prasanth, Manoj C. Raj, H.C. Bajaj, T.H. Kim, R.V. Jasra, Hydrogen sorption in transition metal modified mesoporous materials, Int. J. Hydrogen Energy 35 (6) (2010) 2351–2360.
[11] Y. Chen, H. Lim, Q. Tang, Y.G. Ting Sun, Q. Yan, Y. Yang, Solvent-free aerobic oxidation of benzyl alcohol over Pd monometallic and Au–Pd bimetallic catalysts supported on SBA-16 mesoporous molecular sieves, Appl. Catal. A 380 (2010) 55–65.
[12] V.S. Gutiérrez, A.S. Diez, M. Dennehy, M.A. Volpe, Cu incorporated MCM-48 for the liquid phase hydrogenation of cinnamaldehyde, Microporous Mesoporous Mater. 141 (2011) 207–213.
[13] A.S. Diez, M. Alvarez, M.A. Volpe, Metal-modified mesoporous silicate (MCM-41) material: preparation, characterization and applications as an adsorbent, J. Braz. Chem. Soc. 26 (8) (2015) 1542–1550.
[14] H. Yoshitake, Design of functionalization and structural analysis of organically-modified siliceous oxides with periodic structures for the development of sorbents for hazardous substances, J. Mater. Chem. 20 (2010) 4537–4550.
[15] M.V. Lombardo, M. Videla, A. Calvo, F.G. Requejo, G.J.A.A. Soler-Illia, Aminopropyl-modified mesoporous silica SBA-15 as recovery agents of Cu(II)-sulfate solutions: adsorption efficiency, functional stability and reusability aspects, J. Hazard. Mater. 223 (2012) 53–62.
[16] A. Tsitonaki, B.F. Smets, P.L. Bjerg, Effects of heat-activated persulfate oxidation on soil microorganisms, Water Res. 42 (2008) 1013–1022.
[17] K.C. Huang, R.A. Couttenye, G.E. Hoag, Kinetics of heat-assisted persulfate oxidation of methyl tert-butyl ether (MTBE), Chemosphere 49 (2002) 413–420.
[18] J. Saiena, Z. Ojaghloo, A.R. Soleymani, M.H. Rasoulifard, Homogeneous and heterogeneous AOPs for rapid degradation of Triton X-100 in aqueous media via UV light, nano titania hydrogen peroxide and potassium persulfate, Chem. Eng. J. 167 (2011) 172–182.
[19] S.Y. Yang, P. Wang, X. Yang, L. Shan, W.Y. Zhang, X.T. Shao, R. Niu, Degradation efficiencies of azo dye Acid Orange 7 by the interaction of heat, UV and anions with common oxidants: persulfate, peroxymonosulfate and hydrogen peroxide, J. Hazard. Mater. 179 (2010) 552–558.
[20] Linli Zhu, Zhihui Ai, Wingkei Ho, Lizhi Zhang, Core–shell Fe–Fe_2O_3 nanostructures as effective persulfate activator for degradation of methyl orange, Sep. Purif. Technol. 108 (2013) 159–165.
[21] X.H. Xu, Q.F. Ye, T.M. Tang, D.H. Wang, Hg° oxidative absorption by $K_2S_2O_8$ solution catalyzed by Ag^{+} and Cu^{2+}, J. Hazard. Mater. 158 (2008) 410–416.
[22] F. Ghanbari, M. Moradi, Application of peroxymonosulfate and its activation methods for degradation of environmental organic pollutants: review, Chem. Eng. J. 310 (2017) 41–62.
[23] M.T. Bore, M.P. Mokhonoana, T.L. Ward, N.J. Coville, A.K. Datye, Synthesis and reactivity of gold nanoparticles supported on transition metal doped mesoporous silica, Microporous Mesoporous Mater. 95 (2006) 118–125.
[24] P. Van Der Voort, M. Benjelloun, E.F. Vansant, Rationalization of the Synthesis of

SBA-16: controlling the Micro- and Mesoporosity, J. Phys. Chem. B 106 (2002) 9027–9032.
[25] T. Borrego, M. Andrade, M.L. Pinto, A.R. Silva, A.P. Carvalho, J. Rocha, C. Freire, J. Pires, Physicochemical characterization of silylated functionalized materials, J. Colloid Interface Sci. 344 (2010) 603–610.
[26] Haitao Cui, Ye Zhang, Liangfu Zhao, Yulei Zhu, Adsorption synthesized cobalt-containing mesoporous silica SBA-15 as highly active catalysts for epoxidation of styrene with molecular oxygen, Catal. Commun. 12 (2011) 417–420.
[27] J. Zhong, J. Li, Y. Lu, S. Huang, W. Hu, Oxidation of methyl orange solution with potassium peroxydisulfate, Iran. J. Chem. Chem. Eng. 31 (2012) 21–24.
[28] A.S. Diez, S. Schlichter, V. Tomanech, E.V. Pannunzio Miner, M. Alvarez, M. Dennehy, Spinel manganites synthesized by combustion method: structural characterization and catalytic activity in the oxidative degradation of organic pollutants, J. Environ. Chem. Eng. 5 (2017) 3690–3697.
[29] F.L. Galeener, Band limits and the vibrational spectra of tetrahedral glasses, Phys. Rev. B 19 (1979) 4292–4297.
[30] A. Fidalgo, L. Ilharco, Chemical tailoring of porous silica xerogels: local structure by vibrational spectroscopy, Chem. Eur. J. 10 (2004) 392–398.
[31] J. Pires, M. Pinto, J. Estella, J.C. Echeverría, Characterization of the hydrophobicity of mesoporous silicas and clays with silica pillars by water adsorption and DRIFT, J. Colloid Interface Sci. 317 (2008) 206–213.
[32] G. Socrates, Infrared Characteristic Group Frequencies, 3rd edition, John Wiley and Sons, Chichester, 2001.
[33] I.A. Salem, H.A. El-Ghamry, M.A. El-Ghobashy, Catalytic decolorization of Acid blue 29 dye by H_2O_2 and a heterogeneous catalyst, Beni-Suef Univ. J. Basic Appl. Sci. 3 (2014) 186–192.
[34] Y. Yao, C. Xu, S. Yu, D. Zhang, S. Wang, Facile synthesis of Mn_3O_4–reduced graphene oxide hybrids for catalytic decomposition of aqueous organics, Ind. Eng. Chem. Res. 52 (2013) 3637–3645.
[35] P. Shukla, H.Q. Sun, S.B. Wang, H.M. Ang, M.O. Tadé, Co-SBA-15 for heterogeneous oxidation of phenol with sulfate radical for wastewater treatment, Catal. Today 175 (2011) 380–385.
[36] D. Chen, Y. Li, J. Zhang, J.Z. Zhou, Y. Guo, H. Liu, Magnetic Fe_3O_4/ZnCr-layered double hydroxide composite with enhanced adsorption and photocatalytic activity, Chem. Eng. J. 185 (2012) 120–126.
[37] R. Andreozzi, V. Caprio, A. Insola, R. Marotta, Advanced oxidation processes (AOP) for water purification and recovery, Catal. Today 53 (1999) 51–59.
[38] G.P. Anipsitakis, D.D. Dionysiou, Radical generation by the interaction of transition metals with common oxidants, Environ. Sci. Technol. 38 (2004) 3705–3712.
[39] E. Saputra, S. Muhammada, H. Sun, H.-M. Ang, M.O. Tadé, S. Wang, Manganese oxides at different oxidation states for heterogeneous activation of peroxymonosulfate for phenol degradation in aqueous solutions, Appl. Catal. B 142–143 (2013) 729–735.